Vacuum 169 (2019) 108936

Contents lists available at ScienceDirect

Vacuum

journal homepage: www.elsevier.com/locate/vacuum

Effect of deposition temperature on structure and properties of Nd_2O_3 thin films prepared by magnetron sputtering

Mingyang Shao, Yabo Huang, Jinlong Liu*, Xin Jia, Kan An, Liangxian Chen, Junjun Wei, Chengming Li

Institute for Advanced Materials and Technology, University of Science and Technology Beijing, Beijing, 100083, China

ARTICLE INFO

Keywords:
Nd_2O_3film
Magnetron sputtering
Mechanical properties
Infrared transmission

ABSTRACT

Nd_2O_3 film is a functional film with great potential application value. In this paper, thinNd_2O_3 film was prepared on the surface of Si substrates using RF magnetron reactive sputtering. Nd_2O_3 film with different crystal structures were controlled by changing the deposition temperature. The results show that the Nd_2O_3 film with a cubic structure can be obtained at 150 °C, while a hexagonal structure appears at 250 °C and above. The refractive indices of the cubic and hexagonal Nd_2O_3 films were 1.736 and 2.130, respectively. Moreover, the principle of the influence of deposition temperature on the refractive index of the film was illustrated. The hardness and the elastic modulus of the cubic Nd_2O_3 film were 6.3 GPa and 102 GPa, respectively, which are much lower than the 9.9 GPa and 145 GPa of the hexagonal Nd_2O_3 film. In addition, with a double-sided cubic Nd_2O_3 film, the maximum transmittance of the diamond film reached 87.54%. The results show that the Nd_2O_3 film is an anti-reflection film suitable for optical applications.

1. Introduction

Nd_2O_3 has attractive properties, such as a high dielectric constant, good thermal stability, and excellent optical transmission. Nd_2O_3 particles are often added to ceramic materials to improve their performance as optical [1,2], electrical [3], high temperature superconductors [4] and enhanced coating adhesion [5]. Since the development of the film preparation method, the difficulty of preparing Nd_2O_3 film has been reduced, the quality of the film has been improved, and the applications for Nd_2O_3 film have become more and more extensive. For example, the Nd_2O_3 coating can reduce the oxidation rate and improve the scale adhesion of the steel used to form chromium oxide film [6]. Nd_2O_3 film is an ideal high-k gate oxide in MOS devices with a band gap of 5.8 eV [7] and a theoretical dielectric constant of up to 35 [8]for hexagonal structure. Nd_2O_3 is also used as a superhydrophobic coating on stainless steel surfaces, due to its low electronegativity [9]. Many studies concern the preparation of Nd_2O_3 film. J. X. Wang et al. obtained the Nd_2O_3film with cubic structure using molecular beam epitaxy [10]. Anne Kosola et al. prepared dielectric Nd_2O_3 film using atomic layer deposition [11].S. Chevalier et al. prepared a thin oxide film of Nd_2O_3 using metal organic chemical vapour deposition (MOCVD) to protect the stainless steel from corrosion at high temperatures [6]. Tung-Ming Pan et al. deposited a layer of amorphous Nd_2O_3 film on Si substrate using magnetron reactive sputtering [12] and obtained the desired crystalline structure by annealing the substrate in different atmospheres. Karuppiah Hetherin et al. first deposited a layer of neodymium (Nd)using radio frequency (RF) magnetron sputtering, then used thermal oxidation to obtain a Nd_2O_3 dielectric layer [13]. However, until now, there have been no comprehensive reports on the structural, optical, and mechanical properties of thin Nd_2O_3 films according to preparation processes.

In this paper, Nd_2O_3 films with two different crystal structures were successfully prepared by controlling the deposition temperature. The refractive index and mechanical properties of the Nd_2O_3 film were measured and compared; the results show that Nd_2O_3 has great advantages as an optical film in terms of its mechanical properties and refractive index. It is an ideal anti-reflection film for infrared windows like Ge, ZnS, and CVD diamond. It has been noted that Nd_2O_3 film significantly improves the infrared transmittance of diamond in particular.

2. Experimental procedure

2.1. Sample preparation

The Nd_2O_3 films were deposited on Si(100) substrates using RF

* Corresponding author.
E-mail address: liujinlong@ustb.edu.cn (J. Liu).

https://doi.org/10.1016/j.vacuum.2019.108936
Received 10 July 2019; Received in revised form 3 September 2019; Accepted 8 September 2019
Available online 09 September 2019
0042-207X/

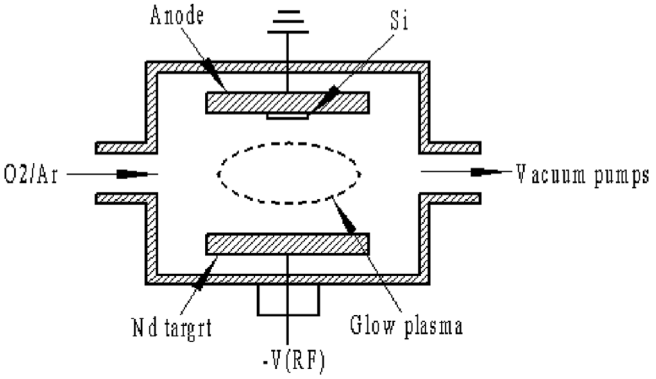

Fig. 1. Schematic view of the vacuum chamber of the RF reactive magnetron sputtering system.

reactive balanced magnetron sputtering [14]. The schematic view of the vacuum chamber is shown in Fig. 1. The Nd metal target, 2 inches in diameter and 99.95% pure, was used with pure O_2 to prepare the Nd_2O_3 film. Argon gas was used to maintain the glow discharge and to provide the main source of ions used to bombard the target. The Si substrate needed to be separately sonicated in acetone and ethanol before it was placed in the chamber. The base pressure of the deposition chamber was 1.0×10^{-4}Pa.Before the film could be prepared, the target was pre-sputtered in an argon atmosphere to remove the surface oxide on the target. The surface of the Si substrate was cleaned using argon plasma. During the experiment, the sputtering power was fixed to 250 W, and the negative bias applied to the substrates was-50 V. The deposition temperature was set to 150 °C, 250 °C, 350 °C, and 450 °C using a resistive heater with feedback control. The chamber temperature was maintained at 100 °C and heated by a resistance wire distributed on the chamber wall. The pre-heat was conducted for more than 6 h to eliminate H_2O in the chamber. During preparation of the film, an appropriate amount of argon and oxygen were introduced to maintain the pressure in the chamber at 0.9 Pa. The 1:10 ratio of O_2 to Ar was controlled by adjusting the mass flow meter.

2.2. Sample characterisation

The crystal structure of the prepared film was characterised using glancing incidence X-ray diffraction (GI-XRD) (TTRIII, Rigaku) with 5° as the angle of incidence. The surface morphology and the roughness of the Nd_2O_3 film were both observed and analysed using atomic force microscopy (Bruker Multimode 8)with a scanned area of $5 \times 5\,\mu m^2$. The density of the film was measured using X-ray reflectance (XRR) (Bruker D8 Advance) with a scanned angle between 0.1 and 5°.Spectroscopic ellipsometry (Sentech, SE 850 DUV) was used to evaluate the optical properties of films in the spectral range of 200–2500 nm at an incidence angle of 70°.The mechanical properties of the film were characterised using nano-mechanical probes (Nano indenterXP), and continuous stiffness was used to measure the hardness and the elastic modulus of the film. Infrared transmittance analysis was performed using Fourier transform infrared spectroscopy (FTIR) (Excalibur 3100,Varian)with a spectral resolution of $8\,cm^{-1}$. The surface chemical state of the film was measured by an X-ray photoelectron spectrometer (XPS) using a ThermoFisher Scientific ESCALAB 250Xi.

3. Results and discussion

3.1. Effect of deposition temperature on deposition rate

Table 1 shows the film thickness and deposition rate of Nd_2O_3 films after deposition for 60 min at various temperatures. These data show the deposition rate with the deposition temperature of the film negative correlation. During the deposition of the film, a low substrate temperature causes the Nd atoms reaching the surface of the substrate to be fixed by the reaction at the position reached without being sufficiently diffused. This deposition could cause pores in the film. Therefore, as the substrate temperature increases, the density of the film was better. Sputtering under the same process parameters, the thickness of the prepared film will decrease as the substrate temperature increases. In addition, a negative bias of 50 V was applied to the surface of the substrate. Therefore, the film on the surface of the substrate was also constantly bombarded by sputter atoms, argon ions, and secondary electrons. Therefore, in the deposition process, not only the formation of a thin film but also desorption phenomenon of deposited atoms after high-energy sputtering atom bombardment exists. As the substrate temperature increases, the deposited atoms have higher activity and the adhesion coefficient decreases [15]. The desorption phenomenon is more serious, so the deposition rate decreases as the substrate temperature increases.

Table 1
Nd_2O_3 film thickness and deposition rate at various deposition temperatures.

Deposition temperature	150 °C	250 °C	350 °C	450 °C
Thickness (nm)	331.87	192.33	185.53	168.41
Deposition rate (nm/min)	5.53	3.21	3.09	2.81

3.2. Thin film structure characterisation

The crystal structure of the Nd_2O_3 film deposited at different temperatures was characterised using XRD; the results are shown in Fig. 2. The diffraction peak position of 28.68°corresponded to the (110) plane of the cubic structure. The diffraction peaks at26.86°, 29.31°, 47.44°, 57.01°, and 64.11°respectivelycorresponded to the (100), (002), (110), (112), and (202) planes of the hexagonal structure. The structure of the film obtained at deposition temperature of 150 °C was cubic; however, when the deposition temperature was 250 °C, 350 °C, and 450 °C, the structure of the film was hexagonal. From the Nd–O binary phase diagram, it can be observed that, under the thermodynamic equilibrium state, Nd_2O_3 almost always exists in the body-centred cubic structure below 860 °C. However, in the magnetron reactive sputtering process, when the deposition temperature was above 250 °C, the hexagonal structure of Nd_2O_3 began to appear in the film. A simplified thermodynamic model can be used to explain the main reason for this phenomenon. In fact, the phase and crystal structure of the reaction product from the magnetron reactive sputtering process mainly depends on

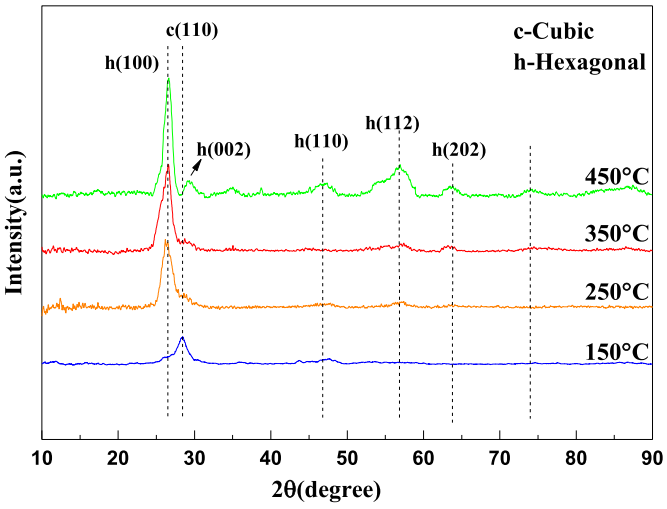

Fig. 2. GI-XRD patterns of Nd_2O_3 film at various deposition temperatures.

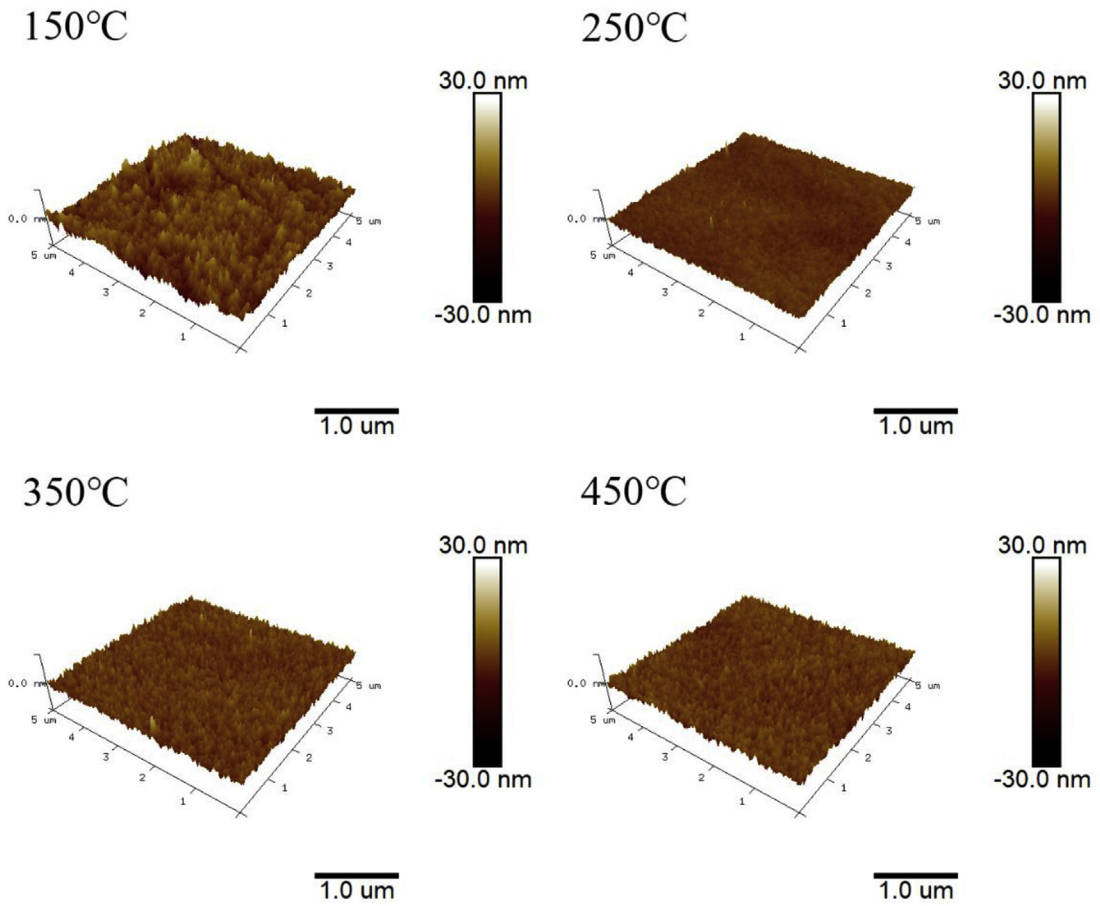

Fig. 3. Surface morphology of Nd_2O_3 film at various deposition temperatures.

the energy of the sputtered particles and the deposition temperature. During the deposition process, the energy of the sputtered particles essentially remained constant. As the heating temperature of the substrate increased, the sum of the energy in the system gradually reached the thermodynamic conditions required to produce hexagonal Nd_2O_3. Thus, the hexagonal structure for Nd_2O_3 appeared in the film. And the cubic structure was gradually reduced.

3.3. Film surface morphology

Fig. 3 is a three-dimensional image of the surface morphology of Nd_2O_3 film prepared at various temperatures. It can be seen that the Nd_2O_3 film prepared at various temperatures are compact and the grain size is at the nanometre level. The surface roughness root mean square (R_{MS}) of the film prepared at 150 °C, 250 °C, 350 °C, and 450 °Cwas4.07 nm, 1.8 nm, 2.86 nm, and 2.85 nm, respectively. It can clearly be seen that the surface roughness of the film prepared at 150 °C is higher than that at 250 °C and higher. The sputtered Nd atoms have the same kinetic energy before reaching the surface of the substrate during the reaction. The deposition temperature determined the surface diffusivity of the Nd atoms. When the deposition temperature waslow (150 °C), the Nd atoms reached the surface of the substrate, the Nd atoms were oxidized to produce Nd_2O_3 by O_2 adsorbed on the surface of the substrate and solidified. When the deposition temperature was raised to 250 °C and above, conditions were favourable for the diffusion of Nd atoms on the surface of the substrate. Thus, a flat film surface was obtained. Meanwhile, as the deposition temperature increased, the deposition rate of the film gradually decreased. Under high temperature conditions, the Nd atoms had sufficient time to diffuse after they reached the surface of the substrate. Therefore, the surface roughness of the film was greatly improved when it was prepared at high temperatures.

3.4. Composition and chemical state

The chemical state of the film surface was analysed by XPS. In order to obtain accurate information, first, the surface of the film is peeled off with an ion gun to remove a small amount of contaminants on the surface. The ion gun has an accelerating voltage of 500 eV and was sputtered on the surface of the film by 60 s. Fig. 4(a) shows the $Nd3d_{5/2}$ XPS spectra of the Nd_2O_3 film. The peak positions of $Nd3d_{5/2}$ in the Nd_2O_3 film prepared at different temperature is 981.2eV, which mainly corresponds to the peak position of the Nd–O bonds. Fig. 4(b) shows the XPS spectra of O1s for Nd_2O_3 films. The O1s core level of the deposited Nd_2O_3 film showed two peaks at 528.0eV and 530.2 eV, which correspond to the Nd–O bonds and the physically adsorbed oxygen [16] in the Nd_2O_3 film, respectively. While for the O1s of standard hydroxide, the peak position is at 531.3 eV [17,18]. Therefore, it could be confirmed that no hydroxide was present in the prepared films.

3.5. Optical properties of the film

Fig. 5 shows the optical refractive index as a function of wavelength for Nd_2O_3 film prepared at various deposition temperatures. The refractive index of the film decreased as the wavelength increased. In particular, the film's refractive index change was abrupt when the deposition temperature increased from 150 °C to 250 °C, increasing the refractive indexfrom 1.736 to 2.028. This is because the structure of the film is different, and the refractive index of the cubic structure is lower than that of the hexagonal structure. When the film structure was

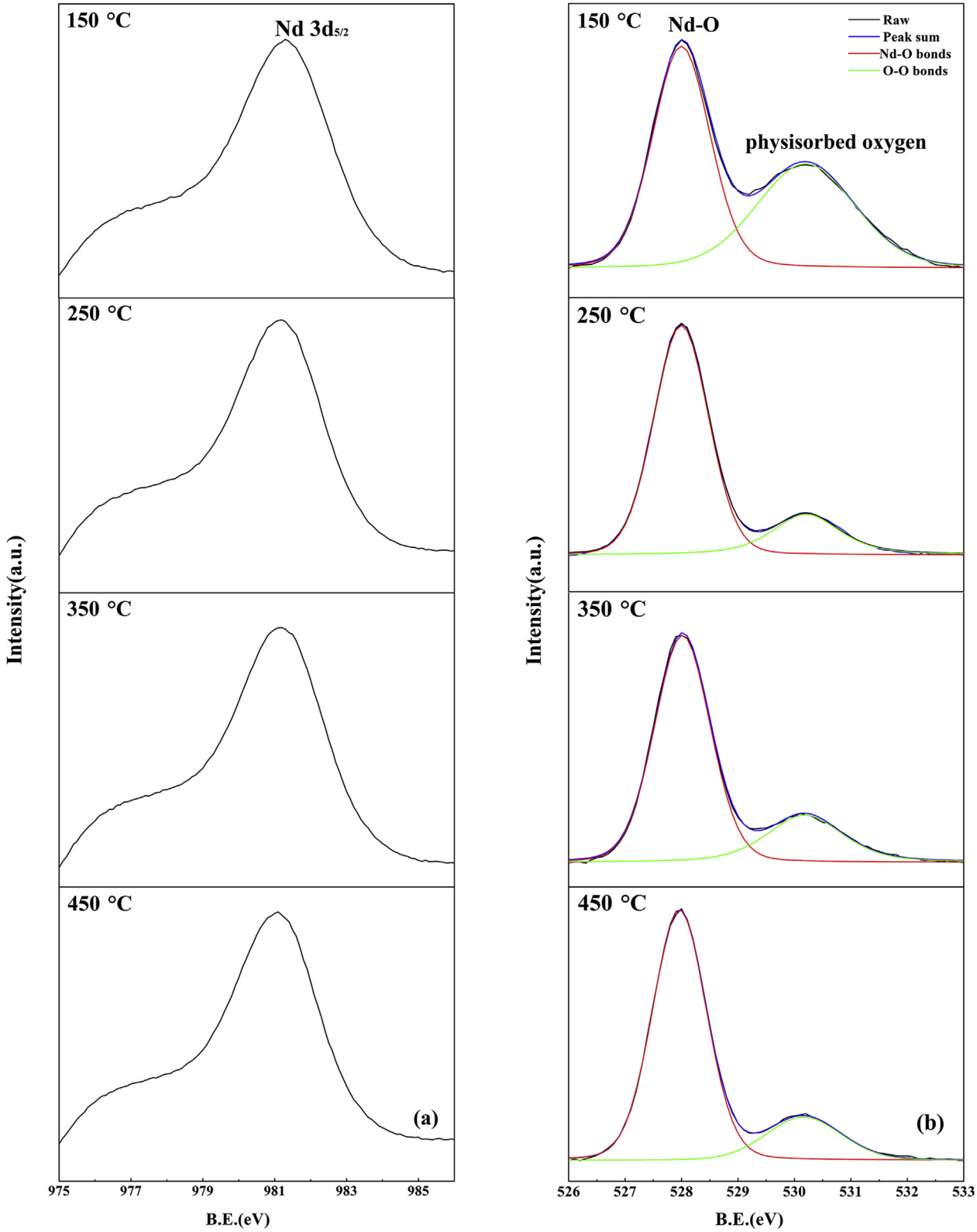

Fig. 4. XPS spectra of Nd_2O_3 films at different deposition temperatures: (a) $Nd3d_{5/2}$ (b) O1s.

uniform, the refractive index of the film increased slightly as the film density increased. It was not difficult to use the Lorentz-Lorenz formulate determine that the refractive index n was positively correlated with ρ [19]:

$$\frac{n^2-1}{n^2+2}=\frac{4\pi}{3}\alpha\rho(1-F)^{-1}$$

The density of the film was measured using XRR, and the corresponding ray reflection curve was presented in Fig. 6. It is considered that a 2 nm SiO2 layer is generally present on the surface of the Si substrate. The $Si/SiO_2/Nd_2O_3$ model was used to simulate the measured

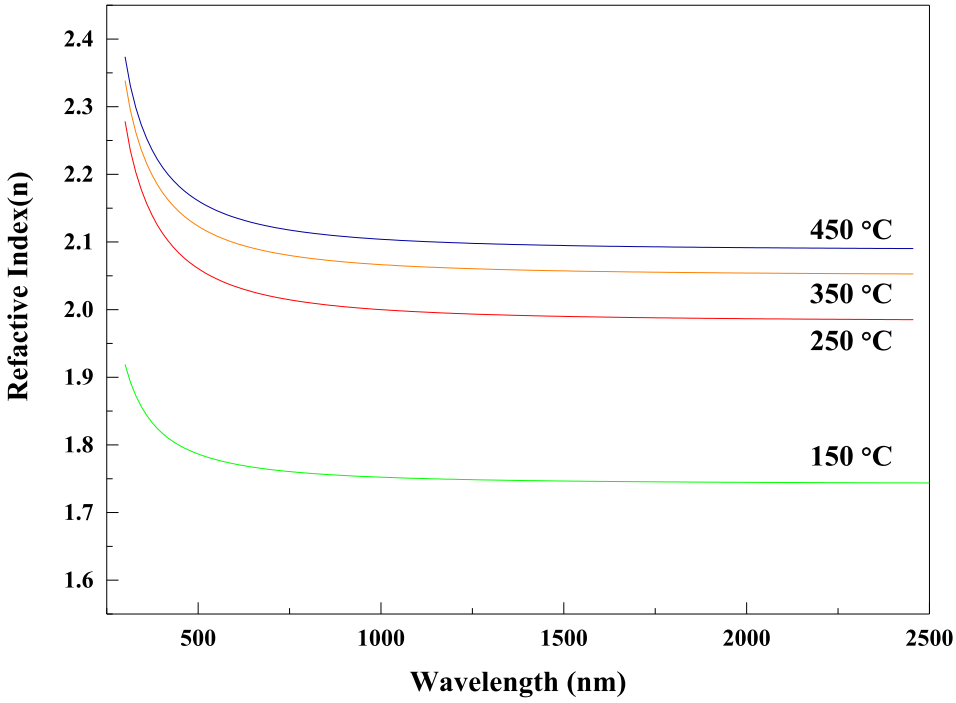

Fig. 5. Refractive index of Nd_2O_3 film at various deposition temperatures.

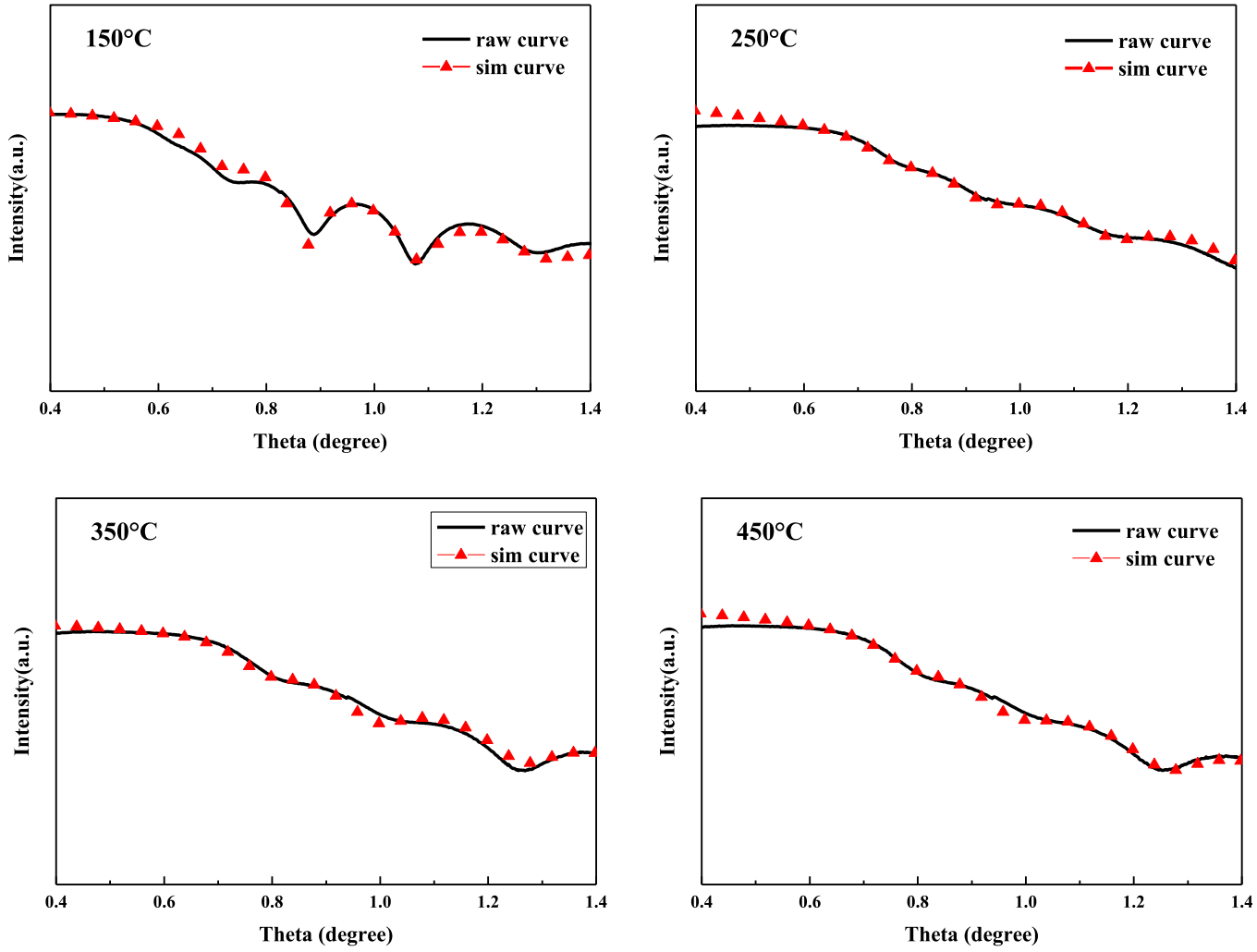

Fig. 6. X-ray reflection (raw and simulated) curves of Nd_2O_3 film at various deposition temperatures.

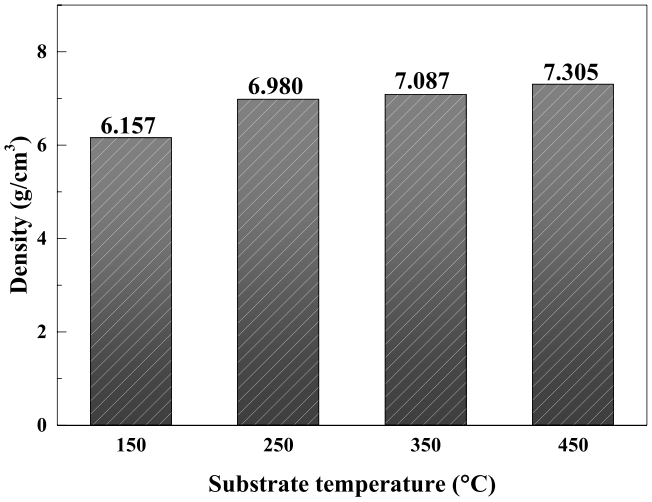

Fig. 7. Density of Nd_2O_3 films at various deposition temperatures.

data. The calculated film density is shown in Fig. 7, and it is clear that the density of the film was greatly improved; as the deposition temperature increased, the diffusion ability of molecules on the surface of the substrate increased during film preparation. At the deposition temperatures of 250 °C, 350 °C, and 450 °C, the hexagonal structure film density gradually increased to 7.305 g/cm^3. This density is very close to the density of the block hexagonal structure of 7.332 g/cm^3. At low deposition temperatures, the critical nucleation radius was small. After the atoms reach the surface of the substrate, the diffusion of the atoms was greatly limited, and thus the resulting film was the structure of the fibers [20]. Moreover, there are many pores between the fiber structures, which is the main reason for the low density of the film at low temperature. As the deposition temperature increases, the diffusion of atoms increases, the pores in the film decrease, and the density of the film gradually increases.

Correspondingly, the refractive index also approached the calculated value of the hexagonal structure [21]. The refractive index of Nd_2O_3 film, whether cubic or hexagonal, is suitable as an anti-reflection film for high refractive index infrared windows, such as Ge, ZnS, and CVD diamond. Therefore, there is great potential for the application of Nd_2O_3 film as optical film.

3.6. Mechanical properties of the film

The mechanical properties of the film were characterised using the continuous stiffness measurement method, and the average values of surface hardness and elastic modulus were calculated. The results are shown in Fig. 8. At 150 °C, the film hardness and the elastic modulus of the Nd_2O_3 film with the cubic structure were 6.3 GPa and 102 GPa, respectively. At a deposition temperature of 250 °C, the hardness and the modulus of the film were greatly improved, becoming 8.7 GPa and 139.01 GPa, respectively. Its hardness and elastic modulus were significantly higher than the Nd_2O_3 film with a cubic structure. Furthermore, the hardness and the modulus of the hexagonal structure Nd_2O_3 film deposited at 350 °C and 450 °C were slightly higher, reaching approximately 9.9 GPa and 145 GP, respectively. As the deposition temperature increased, the film structure gradually changed from cubic to hexagonal, resulting in a gradual increase in the hardness and elastic modulus of the films. Y_2O_3 film is a common optical film with a hardness of 2.69 GPa and an elastic modulus of 29.8 GPa [22,23]. Both mechanical properties of cubic and hexagonal Nd_2O_3 films were higher than that of the Y_2O_3 film, which indicates that Nd_2O_3 film is a good candidate for anti-reflection film.

3.7. Infrared antireflection performance

According to the theoretical design of the diamond anti-reflection film, when the refractive index of the anti-reflection film approaches 1.55 [24], the transmittance of the film system will be high. The cubic structure of Nd_2O_3 has a smaller refractive index than the hexagonal structure, so it is better suited to be optical anti-reflection film for diamonds. Based on a quarter-wavelength anti-reflection design, the film should be the ideal optical thickness D,

$$D = n_{AR} \cdot d_{AR} = \frac{\lambda_0}{4},$$

where n_{AR} is the refractive index of the film, d_{AR} is the film thickness, and λ_0 is the centre wavelength of the anti-reflection film. Generally,

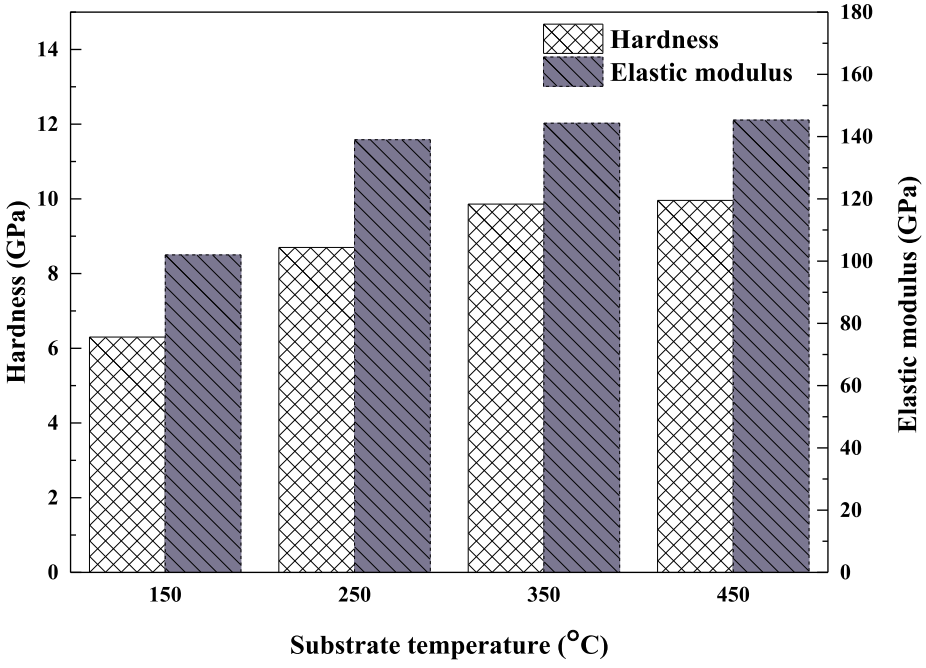

Fig. 8. Mechanical properties of Nd_2O_3 films deposited at various deposition temperatures.

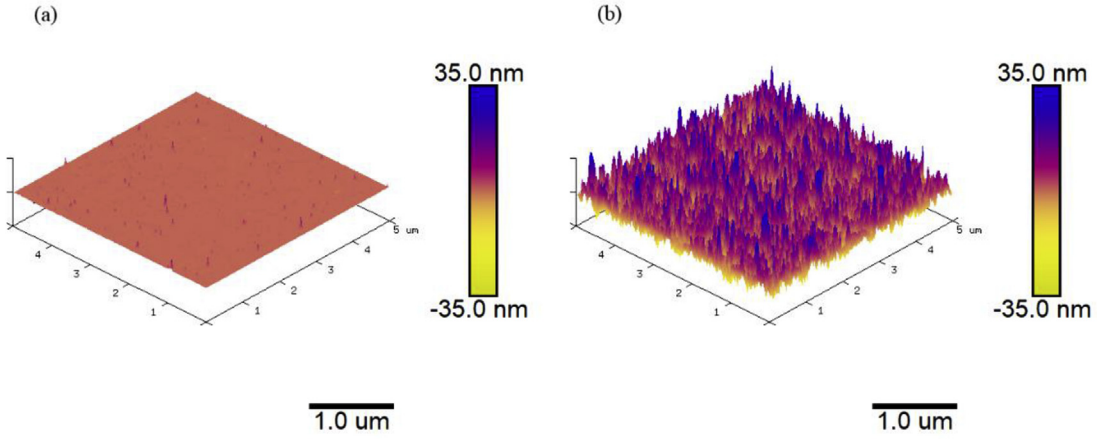

Fig. 9. AFM image of a diamond and a Nd_2O_3/diamond/Nd_2O_3: (a) Diamond substrates; (b) After deposition of Nd_2O_3.

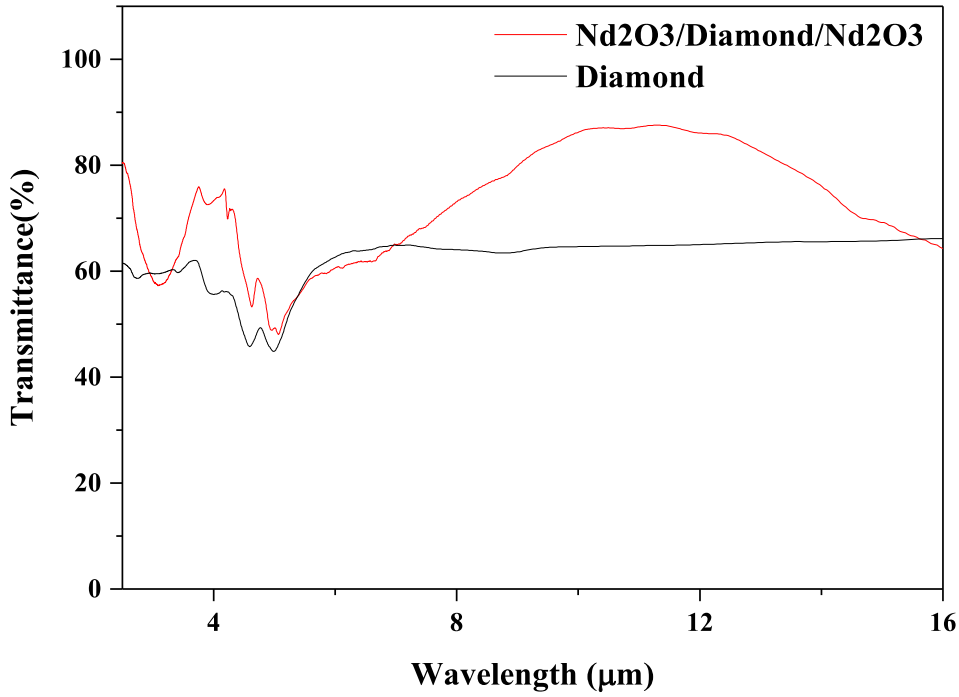

Fig. 10. Transmission spectrum of CVD diamond before and after double-sided deposition of Nd_2O_3.

the application wavelength of diamond is at a wavelength of 8–12 μm and a transmittance of a centre wavelength λ_0 of 10.6 μm. Fig. 9 shows the surface morphology of diamond substrates and Nd_2O_3 film deposited on the diamond substrate at 150 °C.The surface roughness of the diamond substrate was 0.296 nm and the Nd_2O_3 film deposited on the diamond substrate was 7.87 nm.The infrared transmittance of diamond and diamond with double-sided deposition of Nd_2O_3 (Nd_2O_3/diamond/Nd_2O_3) is shown in Fig. 10; it can be observed that the infrared transmittance of the diamond coated with Nd_2O_3 film was significantly higher than that of the uncoated one. At a wavelength range of 8–12 μm, the average transmittance of a diamond without an anti-reflection coating was 64.30%.The average transmittance of diamond with the AR coating was 82.42%, which was 18.12% higher. In particular, at 11.2 μm, the infrared transmittance of Nd_2O_3/diamond/Nd_2O_3 was 87.54%, showing a dramatic anti-reflection effect.

4. Conclusion

Different structures of Nd_2O_3 film were prepared on silicon substrates using magnetron reactive sputtering. When the deposition temperature was 150 °C, the film had cubic structure, but it changed to hexagonal structure when the deposition temperature was higher than 250 °C.The refractive indices of the cubic Nd_2O_3 films were 1.736, and the refractive index of film with a hexagonal structure prepared at higher temperatures gradually increased due to the increase in film density. The hardness and the elastic modulus of the cubic Nd_2O_3 film were 6.3 GPa and 102 GPa, respectively, which were much lower than those of the hexagonal Nd_2O_3 film (which were 9.9 GPa and 145 GPa, respectively). In the infrared band of 8–12 μm, the Nd_2O_3 film deposited on double-sided of the diamond substrate increased the infrared transmittance of the diamond by 22.69%.These results indicate that Nd_2O_3 film is very suitable as an anti-reflection film for high refractive index infrared windows, such as Ge, ZnS, and CVD diamond.

Acknowledgements

This project was supported by the National Key Research and Development Program of China (Grant No.2018YFB0406501) and the

Beijing Municipal Natural Science Foundation (Grant No.4192038). The authors deeply appreciate their financial support.

Appendix A. Supplementary data

Supplementary data to this article can be found online at https://doi.org/10.1016/j.vacuum.2019.108936.

References

[1] R.S. Gedam, D.D. Ramteke, Electrical and optical properties of lithium borate glasses doped with Nd2O3, J. Rare Earths 30 (8) (2012) 785–789.

[2] Y. Yue, C. Shao, S. Kang, F. Wang, X. Wang, J. Ren, D. He, W. Chen, L. Hu, Investigation of luminescence mechanism of Nd3+-doped calcium aluminate glasses: effect of glass-formers, J. Non-Cryst. Solids 505 (2019) 333–339.

[3] A.A. Ali, M.H. Shaaban, Electrical properties of LiBBaTe glass doped with Nd2O3, Solid State Sci. 12 (12) (2010) 2148–2154.

[4] F. Delorme, C. Harnois, I. Monot-Laffez, G. Desgardin, Nd_2O_3 doping oftop-seeding-melt-texture-growth-processed $YBa_2Cu_3O_{7-\delta}$ ceramics, Physica C 372–376 (2002) 1127–1130.

[5] S.G. Song, W. W, S.L. Tan, L.L. Wang, Effect of rare earth doped with Nd_2O_3 on microstructure and properties of YSZ/(Ni, Al) composite coatings, Surf. Technol. 45 (10) (2016).

[6] S. Chevalier, G. Bonnet, J.P. Larpin, Metal-organic chemical vapor deposition of $Cr_2O_3$and Nd_2O_3 coatings. Oxide growth kinetics and characterization, Appl. Surf. Sci. 167 (2000) 125–133.

[7] A. Fissel, Z. Elassar, O. Kirfel, E. Bugiel, M. Czernohorsky, H.J. Osten, Interface formation during molecular beam epitaxial growth of neodymium oxide on silicon, J. Appl. Phys. 99 (7) (2006) 074105.

[8] T. Busani, R.A. Devine, P. Gonon, Structural effects in the dielectric constant of rare-EarthOxides: Nd_2O_3, Ecs Transactions 1 (5) (2005) 11.

[9] S. Zenkin, Š. Kos, J. Musil, G. Rohrer, Hydrophobicity of thin films of compounds of low-electronegativity metals, J. Am. Ceram. Soc. 97 (9) (2014) 2713–2717.

[10] J.X. Wang, A. lahat, A. Fissel, D. Schwendt, Structural and strain relaxation study of epitaxially grown nanothickNd203/Si(111) heterostructure, 2009 4th IEEE International Conference on Nano/Micro Engineered and Molecular Systems, Shenzhen, 2009, pp. 436–440.

[11] A. Kosola, J. Päiväsaari, M. Putkonen, L. Niinistö, Neodymium oxide and neodymium aluminate thin films by atomic layer deposition, Thin Solid Films 479 (1–2) (2005) 152–159.

[12] T.-M. Pan, J.-D. Lee, W.-W. Yeh, Influence of oxygen content on the structural and electrical characteristics of thin neodymium oxide gate dielectrics, J. Appl. Phys. 101 (2) (2007) 024110.

[13] K. Hetherin, S. Ramesh, Y.H. Wong, Effects of thermal oxidation duration on the structural and electrical properties of Nd2O3/Si system, Appl. Phys. A 123 (8) (2017).

[14] D.A. Golosov, Balanced magnetic field in magnetron sputtering systems, Vacuum 139 (2017) 109–116.

[15] N. Xu, Z.T. Liu, W.T. Liu, Y.M. Shen, Deposition ytterbium oxide thin films by RF magnetron sputtering, Rare Metal Mater. Eng. (S3) (2007) 82–85.

[16] P. Lei, J. Zhu, Y. Zhu, C. Jiang, X. Yin, Yttrium oxide thin films prepared under different oxygen-content atmospheres: microstructure and optical properties, Appl. Phys. A 108 (3) (2012) 621–628.

[17] C.D. Wagner, D.E. Passoja, H.F. Hillery, T.G. Kinisky, H.A. Six, W.T. Jansen, J.A. Taylor, Auger and photoelectron line energy relationships in aluminum–oxygen and silicon–oxygen compounds, J. Vac. Sci. Technol. 21 (4) (1982) 933–944.

[18] J.M. Schneider, A. Anders, B. Hjörvarsson, I. Petrov, K. Macák, U. Helmersson, J.-E. Sundgren, Hydrogen uptake in alumina thin films synthesized from an aluminum plasma stream in an oxygen ambient, Appl. Phys. Lett. 74 (2) (1999) 200–202.

[19] D. Beysens, P. Calmettes, Temperature dependence of the refractive indices of liquids: deviation from the Lorentz–Lorenz formula, J. Chem. Phys. 66 (2) (1977) 766–771.

[20] S. Craig, G.L. Harding, Effects of argon pressure and substrate temperature on the structure and properties of sputtered copper films, J. Vac. Sci. Technol. 19 (2) (1981) 205–215.

[21] N. Singh, S.M. Saini, T. Nautiyal, S. Auluck, Electronic structure and optical properties of rare earth sesquioxides (R2O3, R = La, Pr, and Nd), J. Appl. Phys. 100 (8) (2006) 083525.

[22] S.A. Barve, Jagannath, M.N. Deo, R. Kishore, A. Biswas, L.M. Gantayet, D.S. Patil, Effect of argon ion activity on the properties of Y2O3 thin films deposited by low pressure PACVD, Appl. Surf. Sci. 257 (1) (2010) 215–221.

[23] F. Yan, Z.T. Liu, W.T. Liu, Structural and optical properties of yttrium trioxide thin films prepared by RF magnetron sputtering, Vacuum 86 (1) (2011) 72–77.

[24] L.X. Chen, J.L. Liu, Y.N. Feng, X.B. Yan, K. A, J.J. Wei, C.M. Li, Properties and anti-reflection performance of Y_2O_3 films withDifferent crystal structures on diamond, Surf. Technol. 48 (01) (2019) 146–153.